ROYAL SOCIETY
OF CHEMISTRY

PAPER

Check for updates

Novel thiazole derivatives incorporating phenyl sulphonyl moiety as potent BRAFV600E kinase inhibitors targeting melanoma†

Afaf Y. Khormi,[a] Thoraya. A. Farghaly,[bc] Abrar Bayazeed,[c] Youssef O. Al-Ghamdi,[d] Hanan Gaber Abdulwahab ⓘ *[e] and Mohamed R. Shaaban[b]

Novel thiazole derivatives possessing phenyl sulfonyl moiety were designed and synthesized as B-RAFV600E kinase inhibitors based on the clinically-approved anticancer drug, dabrafenib. All target compounds showed significant inhibition of B-RAFV600E kinase enzyme at nanomolar levels. Compounds **7b** and **13a** revealed excellent B-RAFV600E inhibitory activity, superior to that of dabrafenib with IC_{50} values of 36.3 ± 1.9, 23.1 ± 1.2, and 47.2 ± 2.5 nM, respectively. Moreover, the title compounds were much more selective toward B-RAFV600E kinase than B-RAF wild type. In addition, the most potent compounds were further evaluated for their anticancer activity against B-RAFV600E-mutated and wild type melanoma cells. A positive correlation between the cytotoxic activity and selectivity for B-RAF V600E over B-RAF wild type was clearly observed for compounds **7b**, **11c**, **13a**, and **17**. All the screened compounds potently inhibited the growth of WM266.4 melanoma cells with IC_{50} values in the range from 1.24 to 17.1 μM relative to dabrafenib ($IC_{50} = 16.5 \pm 0.91$ μM). Compounds **7b**, **11a** and **11c**, **13a**, and **17** were much more potent than dabrafenib against B-RAFV600E-mutated WM266.4 melanoma cells. Furthermore, compound **7b** suppressed the phosphorylation of downstream ERK1/2 from WM266.4 cells. Also, the docking study revealed the proper orientation and well-fitting of the title compounds into the ATP binding site of B-RAFV600E kinase.

1. Introduction

Ras/Raf/Mek/ERK kinase cascade, also known as MAPK pathway, plays a pivotal role in inter and intracellular communication, which controls the fundamental cellular processes such as cell growth, survival, differentiation, and proliferation.[1,2] This pathway is frequently activated or overexpressed in various disease conditions, particularly cancer.[3,4]

RAF kinases are the key components of Ras/Raf/Mek/ERK pathway. Since their discovery in 1983, RAF kinases have been associated with cancer. Three isoforms (A-RAF, B-RAF, and C-RAF) are known for the RAF kinase family, showing different degrees of biochemical potencies (B-RAF > C-RAF > A-RAF).[5]

[a]Department of Chemistry, Faculty of Science, King Khalid University, Abha, Saudi Arabia

[b]Department of Chemistry, Faculty of Science, Cairo University, Giza 12613, Egypt

[c]Department of Chemistry, Faculty of Applied Science, Umm Al-Qura University, Makkah Almukarramah, Saudi Arabia

[d]Department of Chemistry, College of Science Al-zulfi, Majmaah University, Al-Majmaah 11952, Saudi Arabia

[e]Department of Pharmaceutical Medicinal Chemistry and Drug Design, Faculty of Pharmacy (Girls), Al-Azhar University, Cairo, Egypt. E-mail: hanangaber@azhar.edu.eg

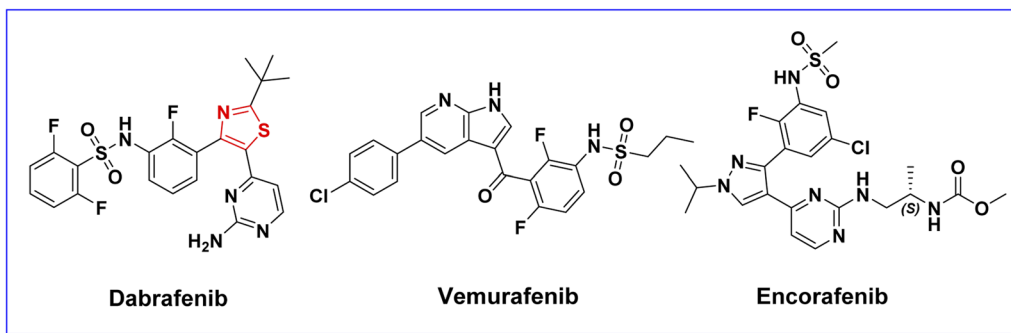† Electronic supplementary information (ESI) available. See https://doi.org/10.1039/d2ra03624j

Being the most frequently mutated isoform in human cancers, B-RAF is the major activating kinase for the MEK/ERK pathway. Numerous activating mutations of B-RAF have been identified by several research groups. Accounting for more than 90% of B-RAF mutations in cancer, B-RAFV600E point mutation in which valine is substituted by glutamic acid in codon 600, is the most common, particularly in melanoma.[6] The overexpression of B-RAFV600E kinase is associated with the proliferation, aggressiveness, and poor prognosis of malignant tumors. In melanoma, B-RAFV600E mutation accounts for 500 times activation relative to the wild-type B-RAF kinase.[6] Therefore, B-RAFV600E kinase is considered as a research hotspot for the discovery of new anticancer agents, and great efforts have been devoted to the development of B-RAFV600E kinase inhibitors.[7,8] As a consequence of this effort, clinically approved B-RAFV600E kinase inhibitors (Fig. 1) have been introduced into the market, resulting in a dramatic change in the treatment of B-RAFV600E-driven cancers, especially melanoma.[9,10] Given that the B-RAF enzyme is crucial for normal cell processes, extensive efforts are currently being made by scientists to obtain potent and safe medications that selectively inhibit B-RAFV600E without interfering with the B-RAF wild-type.[11–13]

On the other hand, the thiazole nucleus has attracted significant attention in medicinal chemistry for the discovery and development of biologically active compounds, particularly

Fig. 1 Clinically-approved B-RAFV600E inhibitors.

anticancer agents.[14–16] Several thiazole-containing compounds have been reported as potent B-RAFV600E kinase inhibitors (Fig. 2).[8,17–23] Moreover, dabrafenib (Fig. 1), a thiazole derivative developed by GlaxoSmithKline as a potent and selective B-RAFV600E inhibitor, was approved by FDA in 2013 for the treatment of B-RAFV600E-driven tumors.[19]

In the light of these facts and in continuation of our effort toward the discovery of potent anticancer agents,[24–36] herein, novel thiazole derivatives were designed and synthesized as potent B-RAFV600E kinase inhibitors with potential anticancer activities, based on the clinically-approved B-RAFV600E inhibitor, dabrafenib. The design of our target compounds is
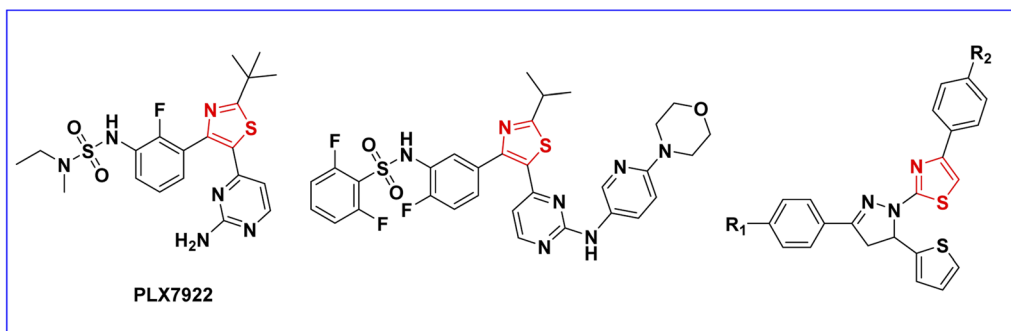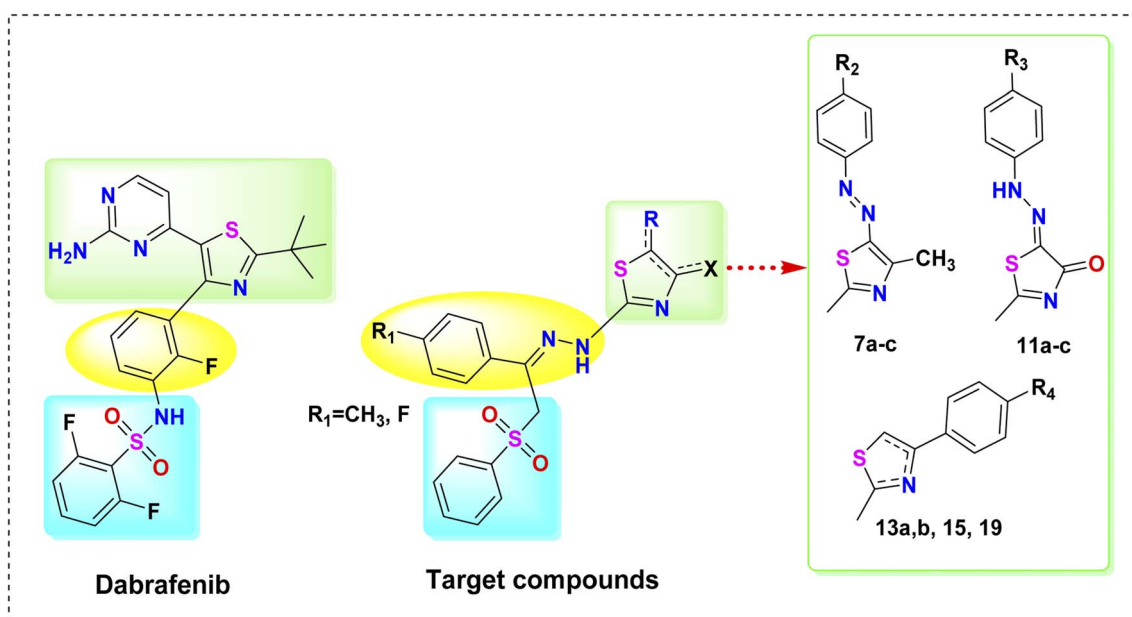

Fig. 2 Reported thiazoles as B-RAFV600E inhibitors.

Fig. 3 Design of the target compounds.

illustrated in Fig. 3. In this work, while conserving the thiazole core of dabrafenib, different moieties were incorporated into the thiazole nucleus, namely, arylazo **7a–c**, arylhydrazono **11a–c**, and aryl groups **13a, b**, **15**, **19**. Motivated by the reported anticancer activity of phenyl sulphonyl derivatives,[30] the 2,6-difluorophenylsulphonamide group of dabrafenib was also replaced by the phenylsulphonylmethyl (PhSO$_2$CH$_2$) moiety. In addition, the fluorophenyl moiety in dabrafenib was replaced by the arylidenehydrazine moiety in the target compounds. Moreover, the substituent effect (R1–R4) on B-RAFV600E kinase inhibitory activity was also explored. On surveying the literature, it was found that bis vemurafenib compounds, reported by Grasso *et al.*,[37] possessed potent B-RAFV600E inhibitory activity in both cell-free and cell-based assays. Also, the anticancer and kinase inhibitory activity of bisthiazole compounds is well established.[38,39] Inspired by these findings, bisthiazole compound **15** was also synthesized to study the effect of dimerization on B-RAFV600E inhibition.

In this work, all target compounds were screened *in vitro* for their ability to inhibit the kinase activity of B-RAFV600E. Furthermore, to evaluate the selectivity of the target compounds, the most active derivatives were tested *in vitro* against B-RAF wild type. The most potent compounds were also screened for their anticancer activity against B-RAFV600E-mutated and B-RAF wild type melanoma cells. Also, a cell-based assay was performed to measure the blocking effect of the title compounds on the phosphorylation of downstream ERK. Finally, a docking study of the most promising compounds was conducted to predict their binding modes within the active site of the B-RAFV600E kinase.

2. Experimental

2.1. Chemistry

The instruments utilized for recording the spectral data are illustrated in the ESI [see ESI† for more details]. The used hydrazonoyl chlorides were prepared by the same method cited in the literature reports.[40,41]
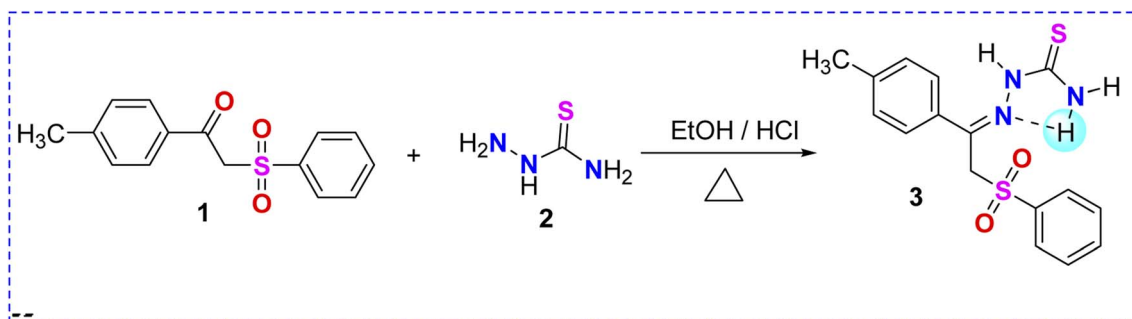
2.1.1. Synthesis of 2-benzenesulfonyl-1-*p*-(substituted phenyl)-ethanone thiosemicarbazone (3 and 17). As usual, in our previous work[24,42] related to the synthesis of thiosemicarbazone derivatives, we synthesized derivatives **3** and **17** through the condensation reaction under reflux of

phenylsulfone derivatives **1** and **16** (0.005 mol) with thiosemicarbazide **2** (0.005 mol) in 15 mL ethanol with drops of conc. HCl. Through the reflux of the reaction, the yellow solid of the two derivatives were precipitated after 10 min, and then the reflux was completed for 2 h. The yellow solid of the two derivatives were collected and crystallized from dioxane.
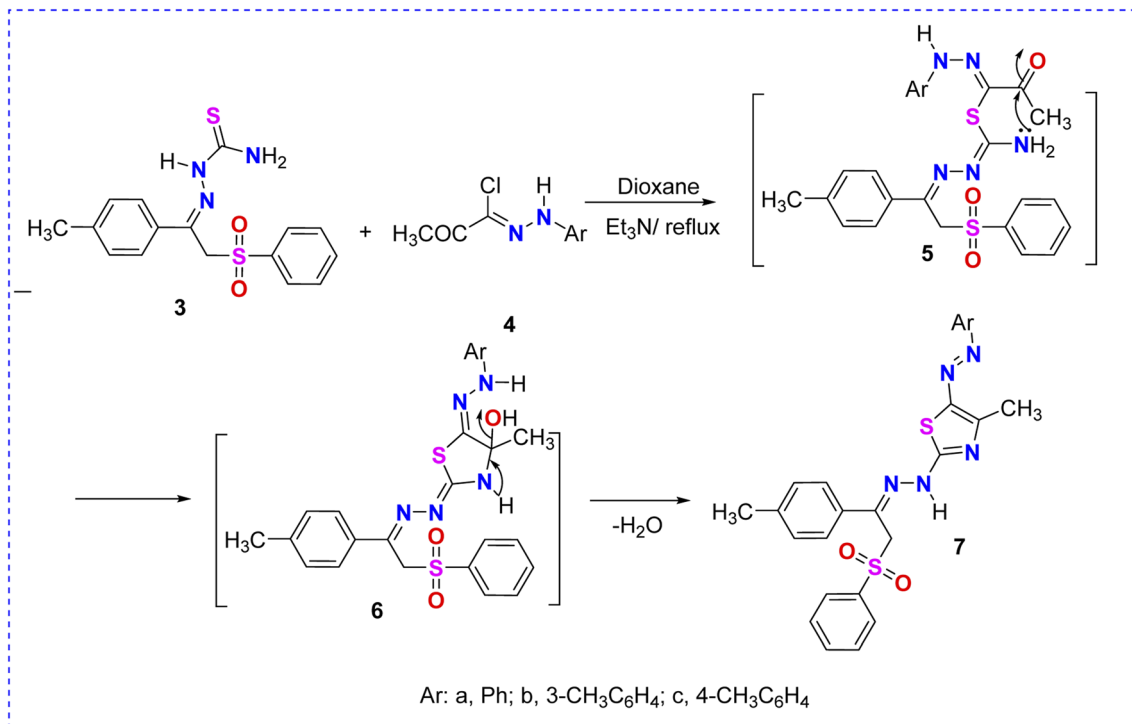
2.1.1.1. 2-Benzenesulfonyl-1-p-tolyl-ethanone thiosemicarbazone (3). Pale yellow solid (86% yield), mp 160–162 °C; IR (KBr) ν_{max} 3417, 3248, 3163 (NH and NH$_2$), 3055, 3001 (sp^2 C–H), 2916 (sp^3 C–H), 1612 (C=N), 1496, 1458, 1427, 1303, 1141, 1080 cm^{-1}; ^{1}H NMR (DMSO-d_6) δ 2.28 (s, 3H, CH$_3$), 5.28 (s, 2H, CH$_2$), 7.07 (d, J = 8.1 Hz, 2H, Ar–H), 7.55–7.85 (m, 5H, Ar–H), 7.86 (d, J = 8.1 Hz, 2H, Ar–H), 7.93 (s, 1H, NH), 8.38 (s, 1H, NH), 10.52 (s, 1H, NH); ^{13}C NMR (DMSO-d_6) δ: 14.2, 51.8, 122.6, 127.9, 129.0, 129.2, 130.7, 134.1, 134.8, 135.3, 139.0, 179.0. MS *m/z* (%) 348 (M$^+$ + 1, 0.36), 347 (M$^+$, 1.3), 192 (9), 147 (7), 117 (100), 115 (40), 105 (17), 91 (35), 77 (60), 65 (21). Anal. calcd for C$_{16}$H$_{17}$N$_3$O$_2$S$_2$ (347.46): C, 55.31; H, 4.93; N, 12.09. Found: C, 55.26; H, 4.81; N, 11.94%.

2.1.1.2. 2-Benzenesulfonyl-1-(4-fluorophenyl)-ethanone thiosemicarbazone (17). White crystals (88% yield), mp 205–207 °C; IR (KBr) ν_{max} 3387, 3317, 3263 (NH and NH$_2$), 3062, (sp^2 C–H), 2970, 2900 (sp^3 C–H), 1604 (C=N), 1504, 1473, 1435, 1303, 1234, 1157, 1141, 1080 cm^{-1}; ^{1}H NMR (DMSO-d_6) δ 5.33 (s, 2H, CH$_2$), 7.05 (t, J = 9 Hz, 2H, Ar–H), 7.55–7.94 (m, 7H, Ar–H), 8.02 (s, 1H, NH), 8.41 (s, 1H, NH), 10.60 (s, 1H, NH); ^{13}C NMR (DMSO-d_6) δ 52.9 (CH$_2$), 115.2, 115.4 (d, ^{2}JCF, 20 Hz), 128.5, 129.7, 130.1, 130.2 (d, ^{3}JCF, 8 Hz), 133.2, 134.7, 135.7, 139.7, 162.3, 164.0 (d, ^{1}JCF, 246 Hz), 179.7 (C=S). MS *m/z* (%) 353 (M$^+$ + 2, 1.2), 352 (M$^+$ + 1, 2.5), 351 (M$^+$, 11), 210 (5), 196 (48), 151 (43), 135 (6), 121 (100), 109 (28), 101 (47), 95 (22), 77 (68). Anal. calcd for C$_{15}$H$_{14}$FN$_3$O$_2$S$_2$ (351.42): C, 51.27; H, 4.02; N, 11.96. Found: C, 51.05; H, 3.94; N, 11.86%.
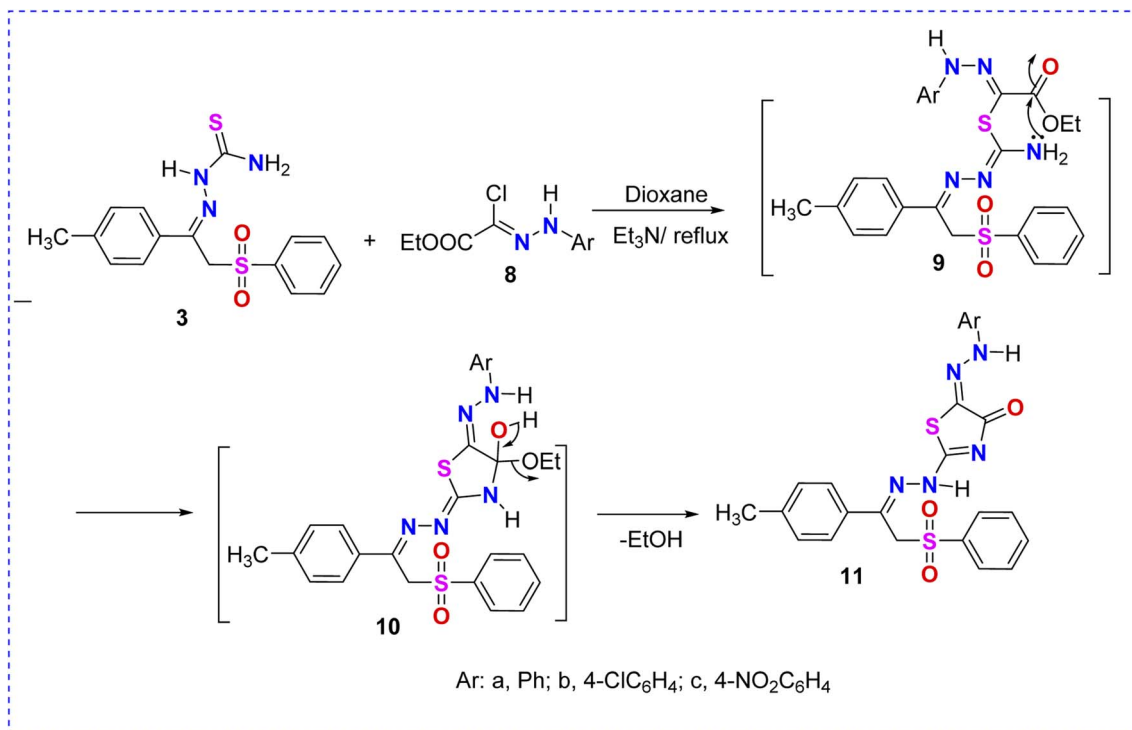
2.1.2. Synthesis of thiazole derivatives 7a–c, 11a–c, 13a and 13b, 15 and 19. In a 100 mL round-bottom flask, substituted phenylsulfone–thiosemicarbazone derivatives **3** or **17** (0.002 mol), according to the listed reactions in Schemes 2–5, were added with the selected hydrazonoyl chlorides **4a–c** or **8a–c**, phenacyl bromide derivatives **12a** and **12b**, **14**, or **18** (0.002 mol) in dioxane were refluxed after the addition of Et$_3$N (0.3 mL) for 5 h. After the reactions were completed, as checked by monitoring with TLC, the colored solids were collected and purified

Scheme 1 Synthesis of the thiosemicarbazone–phenylsulfone derivative **3**.

Scheme 2 Reaction of thiosemicarbazone–phenylsulfone derivative **3** with hydrazonoyl chlorides **4a–c**.
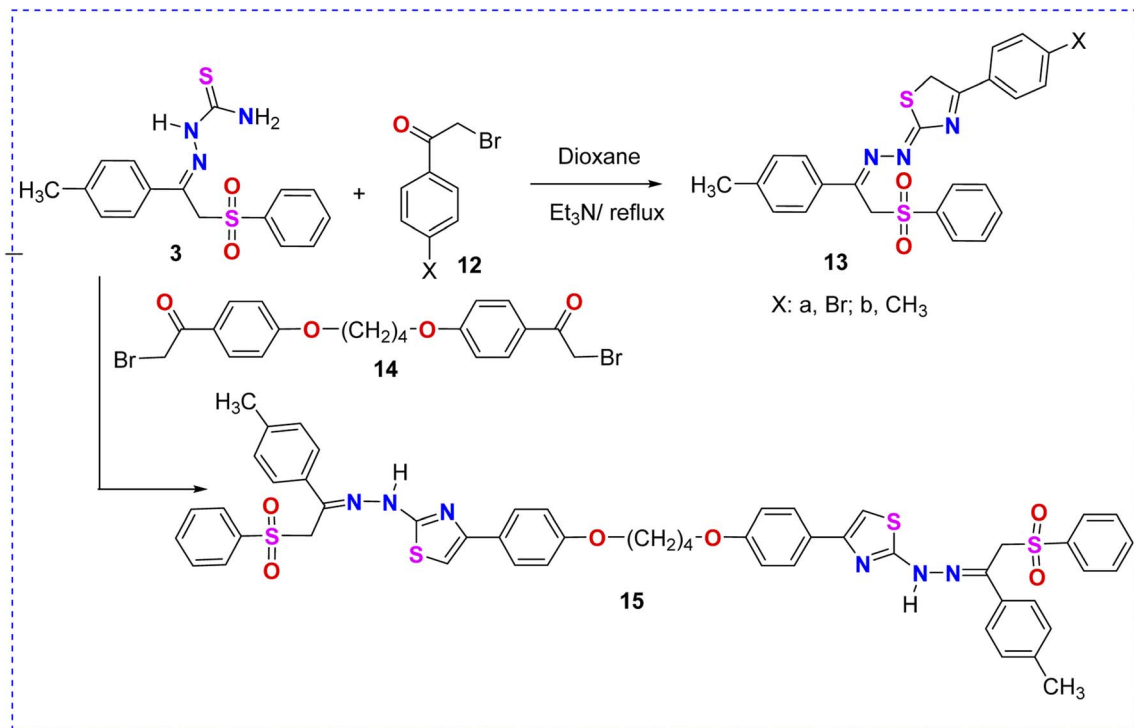

Scheme 3 Reaction of thiosemicarbazone–phenylsulfone derivative **3** with hydrazonoyl chloride **8a–c**.

through crystallization from dioxane to give the thiazole derivatives **7a–c**, **11a–c**, **13a** and **13b**, **15**, and **19**, respectively.

2.1.2.1. N-(2-Benzenesulfonyl-1-p-tolyl-ethylidene)-N′-(4-methyl-5-phenylazo-thiazol-2-yl)-hydrazine (7a). Dark red solid

(82% yield), mp 173–174 °C; IR (KBr) ν_{max} 3255 (NH), 3055, 3001 (sp^2 C–H), 2924 (sp^3 C–H), 1589 (C=N), 1535, 1489, 1411, 1373, 1311, 1242, 1157, 1072 cm^{-1}; ^{1}H NMR (DMSO-d_6) δ 2.35 (s, 3H, CH$_3$), 2.56 (s, 3H, CH$_3$), 5.26 (s, 2H, CH$_2$), 6.65–7.86 (m, 14H, Ar–

Scheme 4 Reaction of thiosemicarbazone–phenylsulfone derivative **3** with phenacyl bromide derivatives **12a**, **12b** and **14**.

Scheme 5 Synthesis of thiosemicarbazone–phenylsulfone derivative **17** and thiazole derivative **19**.

H), 10.67 (s, 1H, NH); ^{13}C NMR (DMSO-d_6) δ: 14.0, 32.1, 53.3, 120.4, 124.2, 127.9, 129.1, 129.5, 131.4, 131.5, 133.8, 134.6, 139.2, 141.9, 152.4, 152.5, 164.2, 166.7, 171.6. MS m/z (%) 490 (M$^+$ + 1, 0.6), 489 (M$^+$, 1.6), 347 (10), 231 (2.7), 143 (2), 117 (74), 105 (6), 92 (12), 91 (37), 77 (100). Anal. calcd for C$_{25}$H$_{23}$N$_5$O$_2$S$_2$ (489.6): C, 61.3; H, 4.7; N, 14.3. Found: C, 61.2; H, 4.6; N, 14.2%.
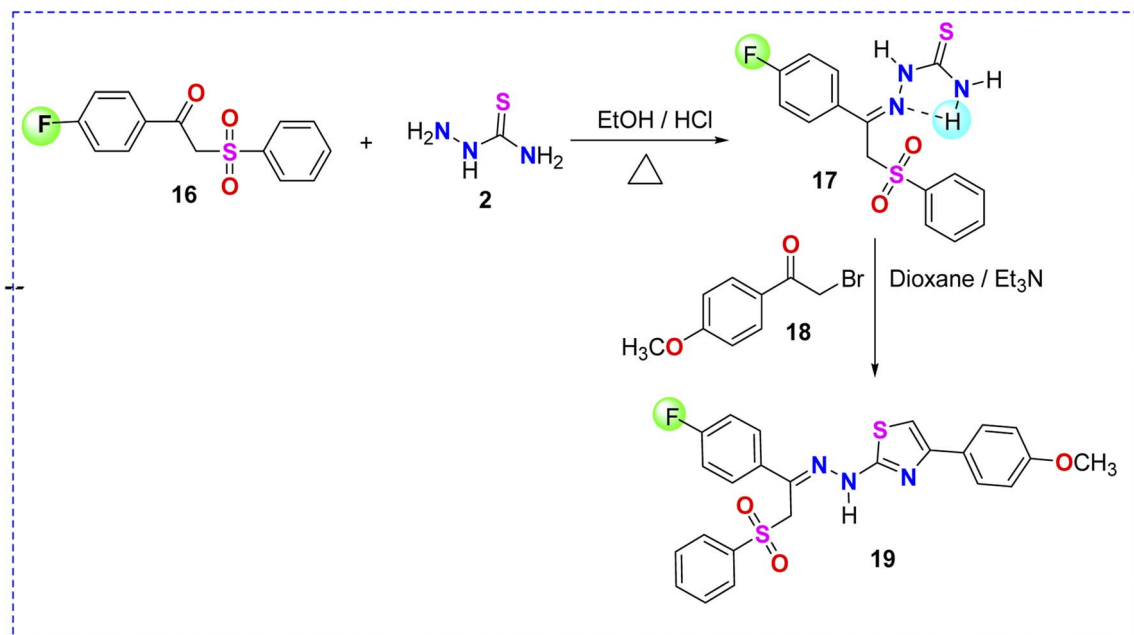
2.1.2.2. N-(2-Benzenesulfonyl-1-p-tolyl-ethylidene)-N'-(4-methyl-5-m-tolylazo-thiazol-2-yl)-hydrazine (7b). Dark red solid (89% yield), mp 148–150 °C; IR (KBr) ν_{max} 3425 (NH), 3032 (sp^2 C–H), 2916 (sp^3 C–H), 1589 (C=N), 1535, 1489, 1373, 1311, 1265, 1188, 1072 cm^{-1}; ^{1}H NMR (DMSO-d_6) δ 2.27 (s, 3H, CH$_3$), 2.34 (s, 3H, CH$_3$), 2.54 (s, 3H, CH$_3$), 5.25 (s, 2H, CH$_2$), 6.78–7.86

(m, 13H, Ar–H), 10.64 (s, 1H, NH); MS m/z (%) 504 (M$^+$ + 1, 1.3), 503 (M$^+$, 4), 362 (12), 161 (2), 142 (11), 132 (10), 117 (64), 106 (31), 91 (100), 77 (89). Anal. calcd for $C_{26}H_{25}N_5O_2S_2$ (503.6): C, 62.0; H, 5.0; N, 13.9. Found: C, 61.9; H, 4.9; N, 13.8%.

2.1.2.3. N-(2-Benzenesulfonyl-1-p-tolyl-ethylidene)-N′-(4-methyl-5-p-tolylazo-thiazol-2-yl)-hydrazine (7c). Red solid (90% yield), mp 180–182 °C; IR (KBr) ν_{max} 3441 (NH), 3032 (sp^2 C–H), 2978, 2924 (sp^3 C–H), 1589 (C=N), 1535, 1481, 1411, 1381, 1311, 1265, 1188, 1072 cm^{-1}; ^{1}H NMR (DMSO-d_6) δ 2.28 (s, 3H, CH$_3$), 2.34 (s, 3H, CH$_3$), 2.55 (s, 3H, CH$_3$), 5.25 (s, 2H, CH$_2$), 6.79–7.85 (m, 13H, Ar–H), 10.65 (s, 1H, NH); ^{13}C NMR (DMSO-d_6) δ: 8.98 (CH$_3$), 21.56 (CH$_3$), 21.79 (CH$_3$), 45.99, 112.33, 115.35, 116.02, 122.89, 128.40, 128.65, 129.54, 129.63, 130.18, 133.01, 134.28, 139.19, 139.81, 143.87, 155.07. MS m/z (%) 504 (M$^+$ + 1, 1.9), 503 (M$^+$, 5.5), 362 (18), 161 (3), 142 (8), 132 (8), 117 (65), 106 (28), 91 (100), 77 (88). Anal. calcd for $C_{26}H_{25}N_5O_2S_2$ (503.6): C, 62.0; H, 5.0; N, 13.9. Found: C, 62.0; H, 5.1; N, 13.9%.

2.1.2.4. 2-[N′-(2-Benzenesulfonyl-1-p-tolyl-ethylidene)-hydrazino]-5-(phenyl-hydrazono)-thiazol-4-one (11a). Yellow solid (72% yield), mp 90–92 °C; IR (KBr) ν_{max} 3425, 3263 (2NH), 3032 (sp^2 C–H), 2985 (sp^3 C–H), 1705 (C=O), 1612 (C=N), 1543, 1496, 1311, 1226, 1157, 1072 cm^{-1}; ^{1}H NMR (DMSO-d_6) δ 2.33 (s, 3H, CH$_3$), 5.21 (s, 2H, CH$_2$), 6.95–7.83 (m, 14H, Ar–H), 10.46 (s, 1H, NH), 12.40 (s, 1H, NH); MS m/z (%) 491 (M$^+$, 10), 350 (8), 120 (14), 117 (91), 105 (13), 92 (39), 91 (55), 77 (100). Anal. calcd for $C_{24}H_{21}N_5O_3S_2$ (491.6): C, 58.6; H, 4.3; N, 14.3. Found: C, 58.5; H, 4.3; N, 14.1%.

2.1.2.5. 2-[N′-(2-Benzenesulfonyl-1-p-tolyl-ethylidene)-hydrazino]-5-[(4-chloro-phenyl)-hydrazono]-thiazol-4-one **(11b).** Yellow solid (71% yield), mp 100–102 °C; IR (KBr) ν_{max} 3417, 3248 (2NH), 2978, 2924 (sp^3 C–H), 1705 (C=O), 1612 (C=N), 1489, 1458, 1311, 1234, 1157, 1080 cm^{-1}; ^{1}H NMR (DMSO-d_6) δ 2.34 (s, 3H, CH$_3$), 5.28 (s, 2H, CH$_2$), 7.06–7.88 (m, 13H, Ar–H), 10.56 (s, 1H, NH), 12.40 (s, 1H, NH); MS m/z (%) 528 (M$^+$ + 2, 1), 527 (M$^+$ + 1, 3), 526 (M$^+$, 10), 142 (11), 129 (13), 117 (91), 115 (41), 111 (25), 91 (44), 83 (24), 77 (100). Anal. calcd for $C_{24}H_{20}ClN_5O_3S_2$ (526.0): C, 54.8; H, 3.8; N, 13.3. Found: C, 54.7; H, 3.7; N, 13.2%.

2.1.2.6. 2-[N′-(2-Benzenesulfonyl-1-p-tolyl-ethylidene)-hydrazino]-5-[(4-nitro-phenyl)-hydrazono]-thiazol-4-one **(11c).** Orange solid (65% yield), mp 180–181 °C; IR (KBr) ν_{max} 3417, 3248 (2NH), 3062 (sp^2 C–H), 2993, 2931 (sp^3 C–H), 1705 (C=O), 1612 (C=N), 1496, 1450, 1327, 1311, 1234, 1149, 1111, 1072 cm^{-1}; ^{1}H NMR (DMSO-d_6) δ 2.29 (s, 3H, CH$_3$), 5.27 (s, 2H, CH$_2$), 7.07–8.40 (m, 13H, Ar–H), 10.52 (s, 1H, NH), 11.18 (s, 1H, NH); ^{13}C NMR (DMSO-d_6) δ: 21.3 (CH$_3$), 46.1 (CH$_2$), 124.5, 126.3, 127.8, 128.0, 128.2, 128.5, 128.5, 128.6, 129.1, 129.5, 129.7, 133.9, 134.6, 136.8, 139.8, 180.0. MS m/z (%) 536 (M$^+$, 2.36), 423 (3), 306 (3), 130 (6), 117 (100), 105 (11), 91 (45), 84 (13), 77 (82). Anal. calcd for $C_{24}H_{20}N_6O_5S_2$ (536.58): C, 53.7; H, 3.8; N, 15.7. Found: C, 53.6; H, 3.5; N, 15.5%.

2.1.2.7. N-(2-Benzenesulfonyl-1-p-tolyl-ethylidene)-N′-[4-(4-bromo-phenyl)-5H-thiazol-2-ylidene]-hydrazine (13a). Pale yellow solid (92% yield), mp 120–121 °C; IR (KBr) ν_{max} 3032 (sp^2 C–H),
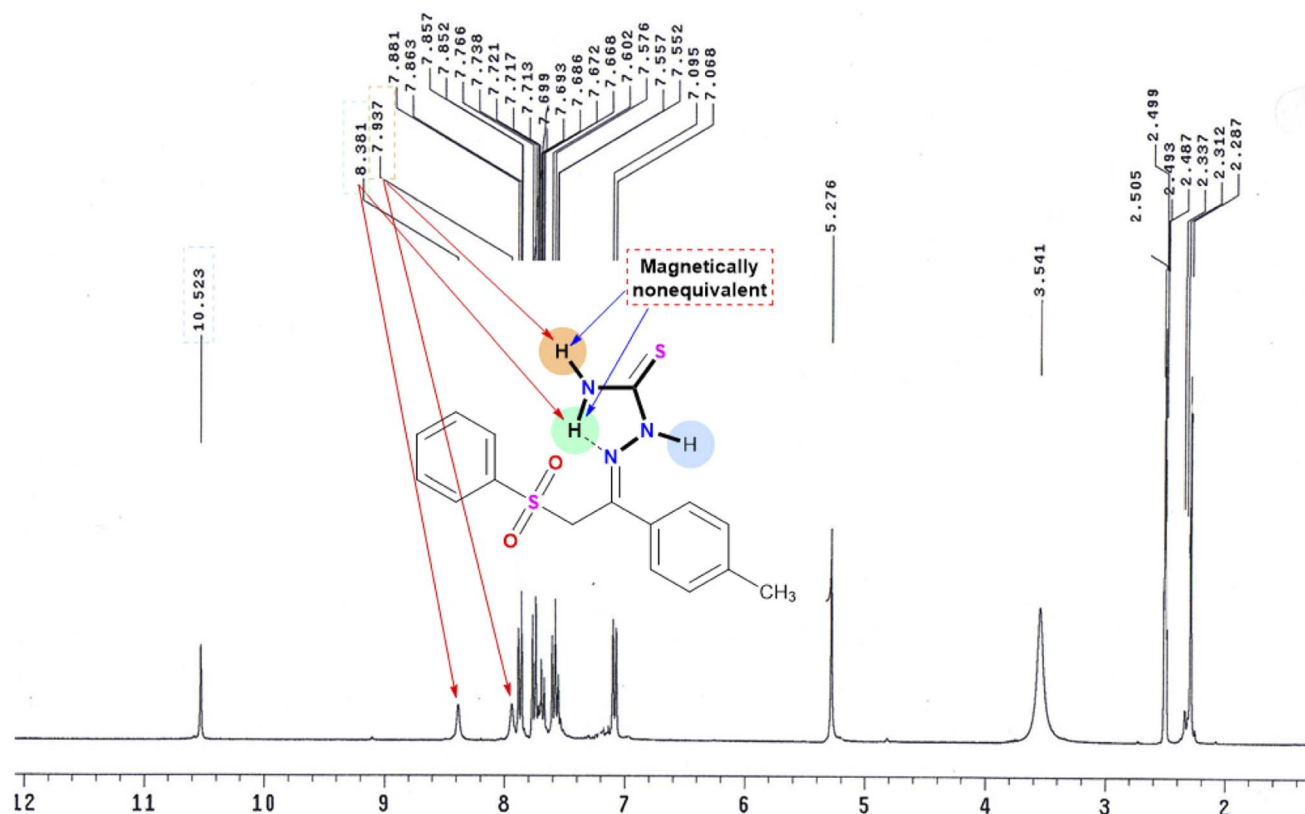

Fig. 4 ^{1}H NMR spectrum and intramolecular hydrogen-bonding of compound **3**.

2954, 2916 (sp^3 C–H), 1604 (C=N), 1489, 1442, 1365, 1311, 1149, 1111, 1080 cm^{-1}; ^{1}H NMR (DMSO-d_6) δ 2.31 (s, 3H, CH$_3$), 5.16 (s, 2H, CH$_2$), 5.18 (s, 2H, CH$_2$), 7.13 (d, J = 7.8 Hz, 2H, Ar–H), 7.54–7.71 (m, 9H, Ar–H), 7.80 (d, J = 7.8 Hz, 2H, Ar–H); MS m/z (%) 527 (M$^+$ + 1, 0.22), 385 (11), 124 (15), 117 (100), 91 (32), 77 (77). Anal. calcd for C$_{24}$H$_{20}$BrN$_3$O$_2$S$_2$ (526.5): C, 54.8; H, 3.8; N, 8.0. Found: C, 54.7; H, 3.7; N, 7.8%.

2.1.2.8. N-(2-Benzenesulfonyl-1-p-tolyl-ethylidene)-N′-(4-p-tolyl-5H-thiazol-2-ylidene)-hydrazine (13b). Pale orange solid (90% yield), mp 178–180 °C; IR (KBr) ν_{max} 3032 (sp^2 C–H), 2954, 2916 (sp^3 C–H), 1604 (C=N), 1504, 1442, 1365, 1311, 1149, 1118, 1080 cm^{-1}; ^{1}H NMR (DMSO-d_6) δ 2.31 (s, 3H, CH$_3$), 2.36 (s, 3H, CH$_3$), 5.16 (s, 2H, CH$_2$), 5.19 (s, 2H, CH$_2$), 7.13 (d, J = 8 Hz, 2H, Ar–H), 7.15 (d, J = 8 Hz, 2H, Ar–H), 7.29 (d, J = 8 Hz, 2H, Ar–H), 7.52–7.65 (m, 5H, Ar–H), 7.73 (d, J = 8 Hz, 2H, Ar–H); MS m/z (%) 462 (M$^+$ + 1, 0.7), 461 (M$^+$, 2.2), 320 (14), 176 (12), 147 (8), 142 (17), 117 (70), 105 (3), 94 (16), 91 (27), 77 (100). Anal. calcd for C$_{25}$H$_{23}$N$_3$O$_2$S$_2$ (461.6): C, 65.1; H, 5.0; N, 9.1. Found: C, 65.0; H, 5.0; N, 9.0%.

2.1.2.9. 1,1′-[1,4-Butanediylbis(oxy)]bis[4-(2-{[2-(benzene-sulfonyl)-1-(p-tolyl)ethylidene]-hydrazino}thiazol-4-yl)benzene] (15). Buff solid (78% yield), mp 185–187 °C; IR (KBr) ν_{max} 3420 (NH), 2939 (sp^3 C–H), 1604 (C=N), 1550, 1512, 1303, 1242, 1157,

1049 cm^{-1}; ^{1}H NMR (DMSO-d_6) δ 1.91 (br.s, 4H, 2CH$_2$), 2.30 (s, 6H, CH$_3$), 4.10 (br.s, 4H, 2CH$_2$), 5.18 (s, 4H, CH$_2$), 6.99 (d, J = 8 Hz, 4H, Ar–H), 7.13 (d, J = 8 Hz, 4H, Ar–H), 7.61 (s, 2H, 2thiazole-H), 7.54–7.89 (m, 18H, Ar–H), 11.60 (br.s, 2H, 2NH); MS m/z (%) 982 (M$^+$ + 1, 0.52), 981 (M$^+$, 1), 256 (2), 139 (5), 117 (21), 110 (21), 98 (22), 91 (20), 84 (42), 77 (31). Anal. calcd for C$_{52}$H$_{48}$N$_6$O$_6$S$_4$ (981.2): C, 63.7; H, 4.9; N, 8.6. Found: C, 63.4; H, 4.9; N, 8.4%.

2.1.2.10. N-[2-Benzenesulfonyl-1-(4-fluorophenyl)-ethylidene]-N′-[4-(4-methoxyphenyl)thiazol-2-yl]-hydrazine (19). Green solid (86% yield), mp 145–147 °C; IR (KBr) ν_{max} 3271 (NH), 3062 (sp^2 C–H), 2939 (sp^3 C–H), 1604 (C=N), 1558, 1512, 1442, 1311, 1242, 1157, 1080 cm^{-1}; ^{1}H NMR (DMSO-d_6) δ 3.79 (s, 3H, OCH$_3$), 5.23 (s, 2H, CH$_2$), 6.98–7.88 (m, 14H, Ar–H and thiazole-H), 11.75 (s, 1H, NH); MS m/z (%) 483 (M$^+$ + 2, 0.36), 481 (M$^+$, 1), 339 (14), 310 (10), 142 (10), 121 (100), 101 (44), 95 (19), 77 (82). Anal. calcd for C$_{24}$H$_{20}$FN$_3$O$_3$S$_2$ (481.6): C, 59.9; H, 4.2; N, 8.7. Found: C, 59.7; H, 4.1; N, 8.7%.

2.2. Biological activity

2.2.1. B-RAF kinase assay. The kinase inhibitory activity of the B-RAF enzyme was measured using B-RAF (wild-type) and B-RAF(V600E) Kinase Assay Kits (BIOSCIENCE). The B-RAF Assay
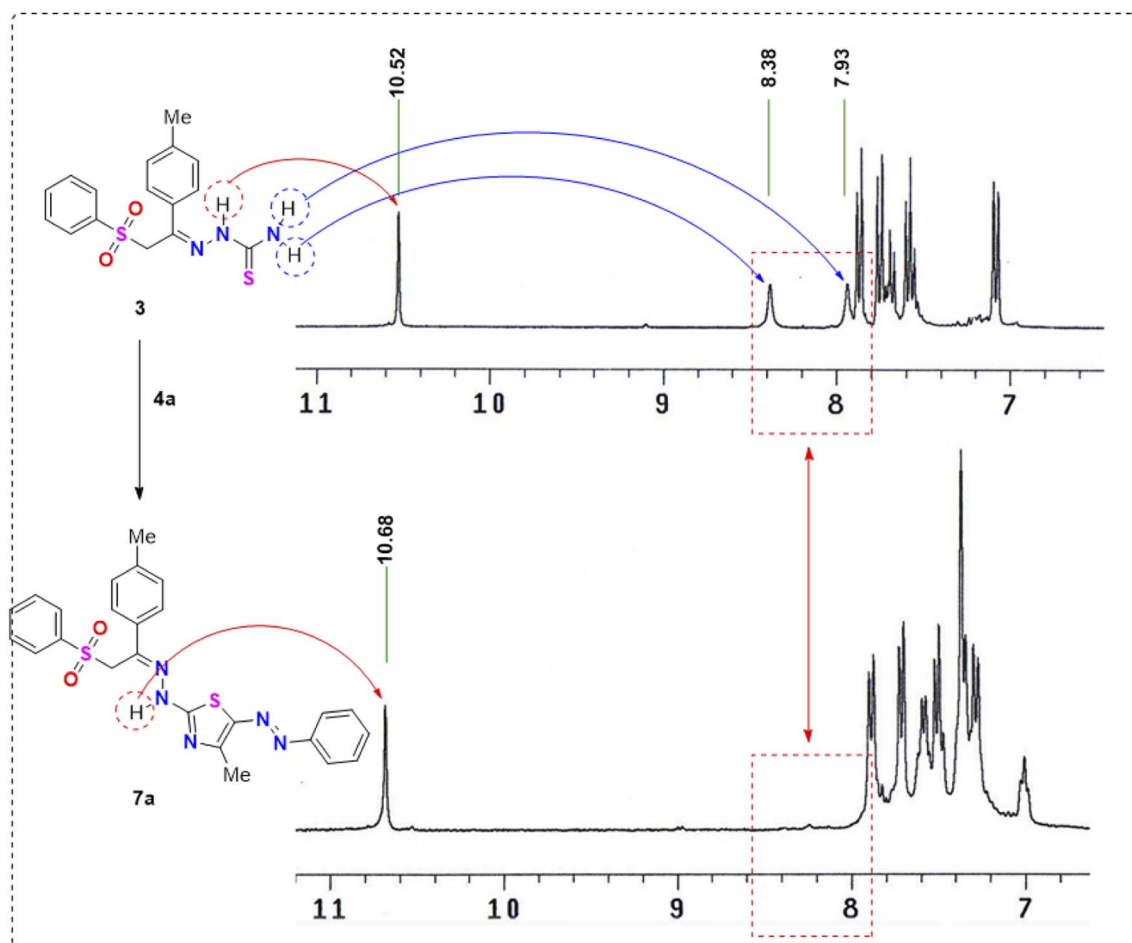

Fig. 5 Comparison of the downfield region of the ^{1}H NMR spectra of the reactant thiosemicarbazone **3** and its product **7a**.

Kit measures the B-RAF kinase activity using Kinase-Glo® MAX as a detection reagent.[43,44] The percentage of inhibition was calculated by equating the investigated phenylsulfone–thiazole derivatives to the control. The values of IC_{50} were calculated from the curve of concentration-inhibition response with ($n = 3$) compared to the reference (dabrafenib) drug.

2.2.2. Cytotoxicity assay. The cytotoxic activity of the phenylsulfone–thiazole derivatives was estimated using the MTT assay.[45] Dabrafenib was used as the reference drug. In the laboratory MTT test group, Sigma was used. In summary, WM266.4 and Sk-mel-23 melanoma cells were grown in DMEM with the added penicillin, FBS, and streptomycin, and were retained with less than 5% CO_2 at 37 °C. Different concentrations of the phenylsulfone–thiazole derivatives to the cells were incubated at 37 °C for 48 h, followed by the addition of the MTT reagent to the cells and re-incubation. At a wavelength = 590 nm, the absorbance was recorded using a plate reader and the cell viability was calculated. IC_{50} was extracted from the concentration inhibition response curve ($n = 3$).

2.2.3. Cell-based B-RAFV600E kinase assay. The blocking effect of title compounds, represented by compound **7b**, on the phosphorylation of downstream ERK in B-RAFV600E-mutated WM266.4 melanoma cells was measured using the ELISA kit (Abcam's ERK1/2 (pT202/Y204) and ERK1/2 (Total) *in vitro* Simple Step ELISA™ Kit). This kit employs an affinity tag-labeled capture antibody and a reporter-conjugated detector antibody, which immunocaptured the sample analyte in solution. Briefly, the cells in the culture medium were treated with compound **7b** and dabrafenib dissolved in DMSO. The expression of phosphorylated ERK (pERK) in the samples was measured (ng mL^{-1}) as duplicate determinations, and the data were compared with dabrafenib as the standard B-RAFV600E kinase inhibitors (for more details, see ESI†).

3. Results and discussion

3.1. Chemistry

The synthesis of the unreported thiosemicarbazone **3** was achieved by the acid-catalyzed condensation of the phenacyl phenyl sulfone derivative **1** with thiosemicarbazide **2** in acidic ethanol, as shown in Scheme 1. The synthesized phenyl sulfone–thiosemicarbazone derivative **3** was further analyzed using spectroscopic techniques. The standard NMR techniques were utilized for assigning all the protons as well as carbons in its structural frame (Scheme 1).

The ^{1}H NMR spectrum for phenyl sulfone–thiosemicarbazone **3** in dimethylsulfoxide-d_6 is described in Fig. 4. The ^{1}H NMR spectrum of thiosemicarbazone **3** revealed the presence of the open-chain thioamide-tautomer with the NH$_2$ protons being partially affected due to the outspread conjugation as well as the presence of the phenylsulfonylmethylene moiety. It was observed that the two protons of the amino group (NH$_2$) were magnetically non-equivalent, displaying two different chemical shift values at $\delta = 7.9$ and 8.4 ppm. This observation could be explained in terms of intramolecular hydrogen bond that restricted or slowed down rotation around the N–C bond.[46,47] It is worth mentioning that the chemical shift values observed for all the NH protons in the presence of phenylsulfonylmethylene group showed a downfield shift of approximately +0.40 to +1.3 ppm compared to the previously reported analog lacking phenylsulfonylmethylene group.[48] Also, the ^{13}C NMR spectrum of the carbothioamide derivative **3** showed a signal at $\delta = 179$ ppm assigned to the C=S group, in addition to another signal at $\delta = 139$ ppm corresponding to C=N.

Thiosemicarbazone **3** was reacted with hydrazonoyl halides **4a–c** as cyclization reagents in dioxane/Et$_3$N to afford the corresponding substituted phenylsulfone–thiazoles **7a–c** pendant to the arylazo substituents (Scheme 2). The IR spectra of derivatives **7a–c** revealed the demise of the NH$_2$ absorption bands of the starting thiosemicarbazone as well as the carbonyl (C=O) group of the reacted hydrazonoyl chlorides. Compared to the ^{1}H NMR spectrum of the starting phenylsulfone–thiosemicarbazone **3**, thiazole derivative **7a** (taken as an example) revealed the disappearance of the magnetically-nonequivalent protons of NH$_2$. Also, the ^{1}H NMR spectrum of arylazothiazole derivative **7a** displayed remarkable four singlet signals at $\delta = 2.38, 2.59, 5.28,$ and 10.86 corresponding to two CH$_3$, CH$_2$, and

Table 1 Kinase assay of B-RAF (V600E and wild-type) and cytotoxicity assay of the target compounds

Compound no.	B-RAF (V600E) (nM)	B-RAF (wild type) (nM)	WM266.4^a (μM)	Sk-mel-23^b (μM)
3	115.3 ± 6	—^{c}	—	—
7a	198.6 ± 10	—	—	—
7b	36.3 ± 1.9	123.5 ± 6.6	3.18 ± 0.17	7.87 ± 0.40
7c	108.4 ± 5.6	—	—	—
11a	84.9 ± 4.4	361.1 ± 19.4	6.18 ± 0.34	0.43 ± 0.02
11b	185.2 ± 9.6	—	—	—
11c	95.4 ± 5	229 ± 12.3	1.53 ± 0.08	22.3 ± 1.14
13a	23.1 ± 1.2	97.9 ± 5.2	4.52 ± 0.25	50.2 ± 2.56
13b	205.6 ± 11	—	—	—
15	51.9 ± 2.7	251.2 ± 13.5	17.1 ± 0.94	17.6 ± 0.89
17	68.2 ± 3.5	153 ± 8.2	1.24 ± 0.07	12.4 ± 0.63
19	116.3 ± 8	—	—	—
Dabrafenib	47.2 ± 2.5	231.2 ± 12.4	16.5 ± 0.91	9.03 ± 0.46

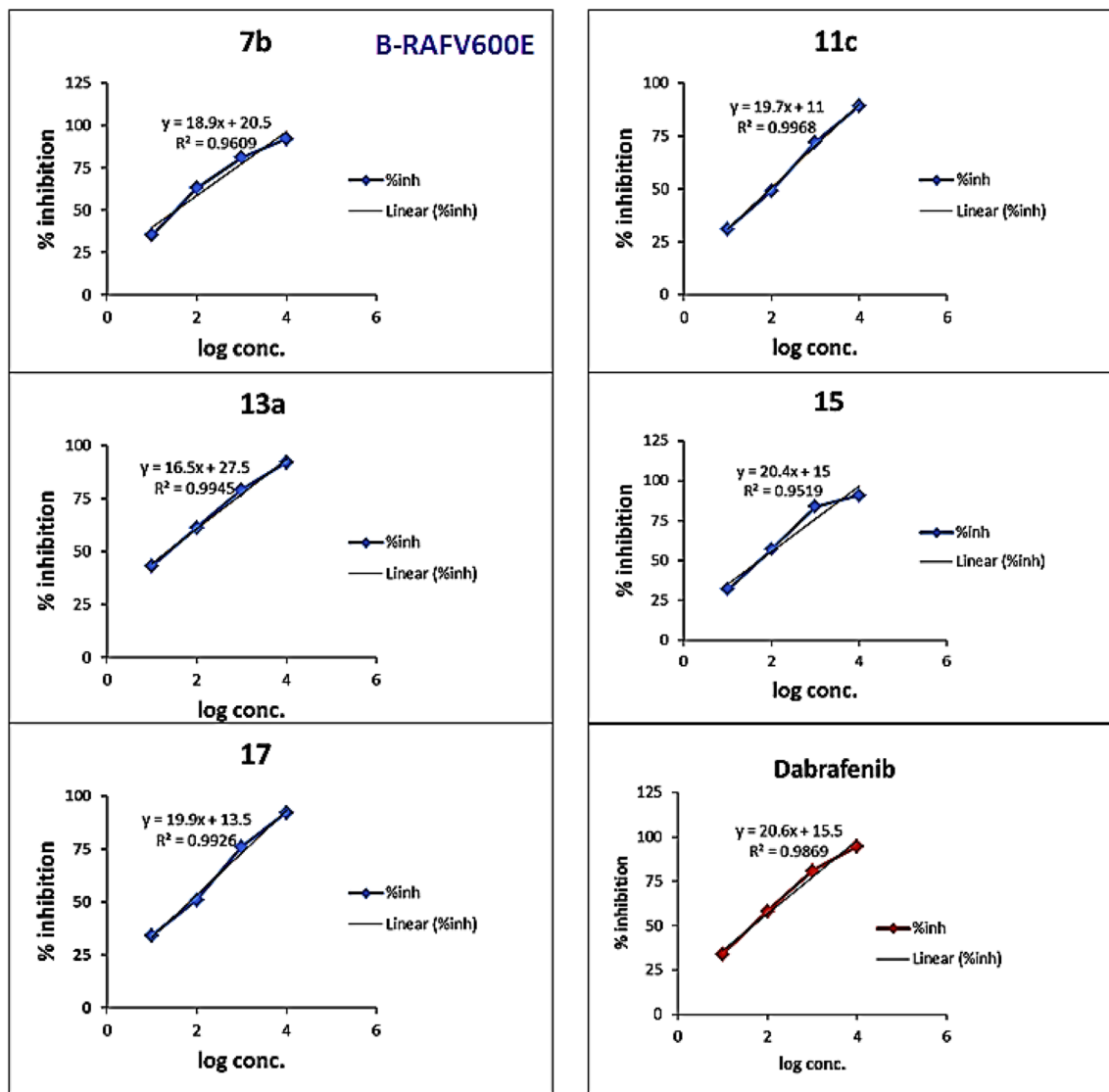^{a} B-RAFV600E-mutated WM266.4 melanoma cells. ^{b} B-RAF wild type Sk-mel-23 melanoma cells. ^{c} Not determined.

© 2022 The Author(s). Published by the Royal Society of Chemistry

Fig. 6 *In vitro* B-RAFV600E assay curves of compounds **7b**, **11c**, **13a**, **15**, **17**, and dabrafenib.

NH protons, respectively, in addition to fourteen aromatic protons in the δ range of 7.27–7.87 ppm (Scheme 2 and Fig. 5).

In a similar manner, the reactivity of thiosemicarbazone **3** toward *C*-1-(ethoxycarbonyl)-*N*-4-arylhydrazonoyl chlorides **8a–c** was investigated. Thus, the reaction of (**3**) with halogenated reagents **8a–c** in dioxane afforded the corresponding arylazo-thiazolone derivatives **11a–c**, as shown in Scheme 3. The suggested structures of compounds **11a–c** were confirmed based on the data extracted from their spectral analyses (Scheme 3).

The reaction of 2-(2-(phenylsulfonyl)-1-(*p*-tolyl)ethylidene)hydrazine-1-carbothioamide (**3**) with α-bromocarbonyl derivatives **12a** and **12b** in dioxane/Et$_3$N furnished the corresponding phenylsulfone–thiazoles **13a** and **13b**, as illustrated in Scheme 4. The ^{1}H NMR spectrum of derivative **13a** showed three singlet signals at δ 2.31, 5.16, and 5.18 ppm assigned to the methyl and two methylene protons, respectively. Moreover, multiplet signals of the thirteen aromatic protons appeared in the region of δ 7.13–7.80 ppm. Molecular weights (*m/z*) of phenylsulfone–

thiazole derivatives **13a** and **13b**, extracted from their mass spectra, were identical with the calculated values (Scheme 4).

The treatment of 2-(2-(phenylsulfonyl)-1-(*p*-tolyl)ethylidene)hydrazine-1-carbothioamide (**3**) with the interesting *bis*-α-bromocarbonyl derivative **14** in dioxane/Et$_3$N afforded the corresponding bis-phenylsulfone–thiazole derivative **15**, as depicted in Scheme 4. The ^{1}H NMR spectrum of **15** revealed two singlet signals at δ 2.30 and 5.18 ppm assigned to the methyl and methylene protons, respectively. The protons of the four methylene (CH$_2$) groups of the aliphatic ether spacer were confirmed at δ = 1.90 and 4.10 ppm. In addition, the aromatic protons as well as the thiazole-5H signals were detected in the region of δ 6.99–7.89 and 7.61 ppm, respectively.

Prompted by the role of fluorine atom in enhancing the biological activity of previously reported fluorinated compounds,[49,50] *p*-fluorophenacyl sulfone **16** was reacted with thiosemicarbazide **2** in ethanolic solution containing HCl to obtain the corresponding thiosemicarbazone derivative **17**
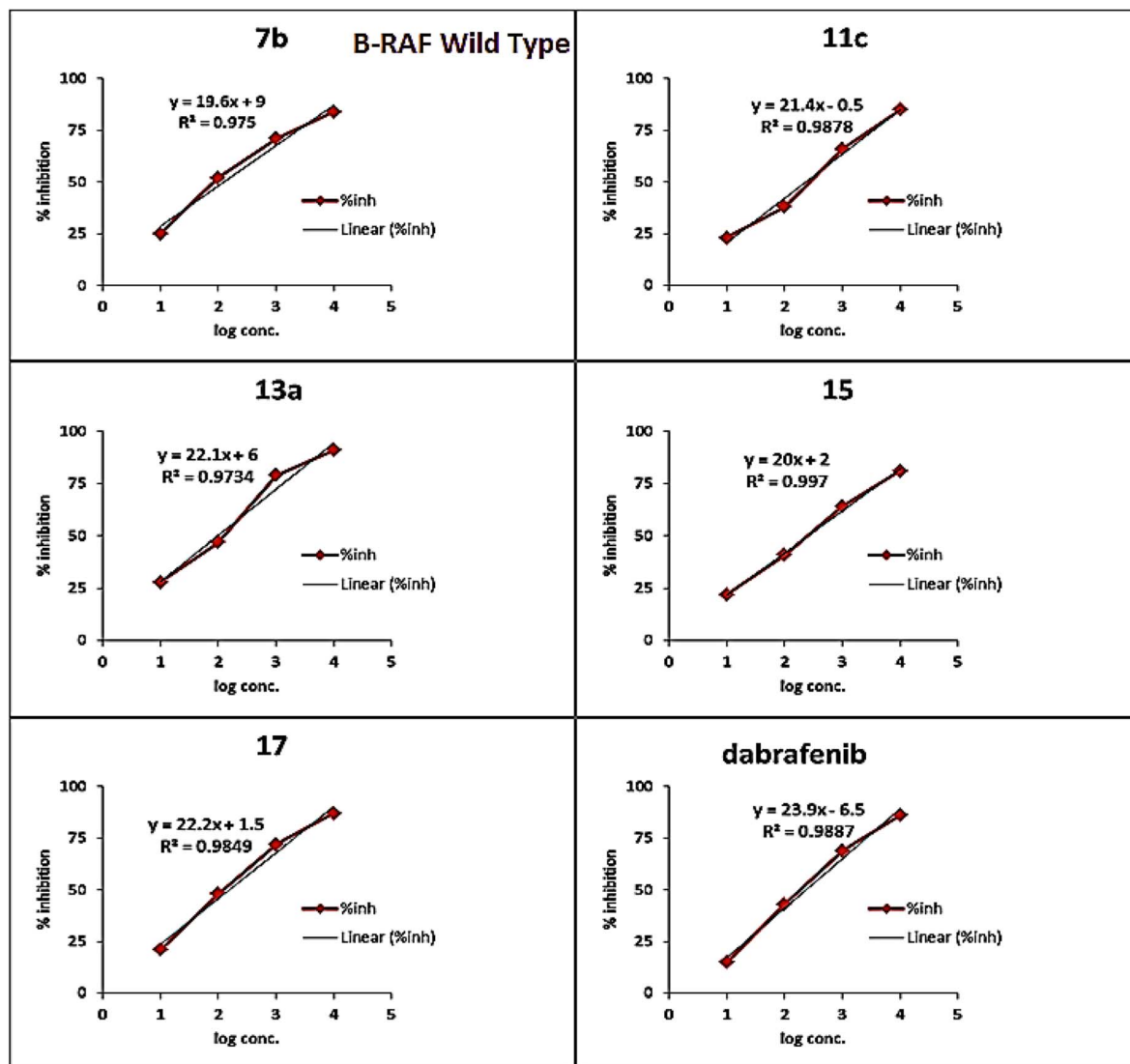
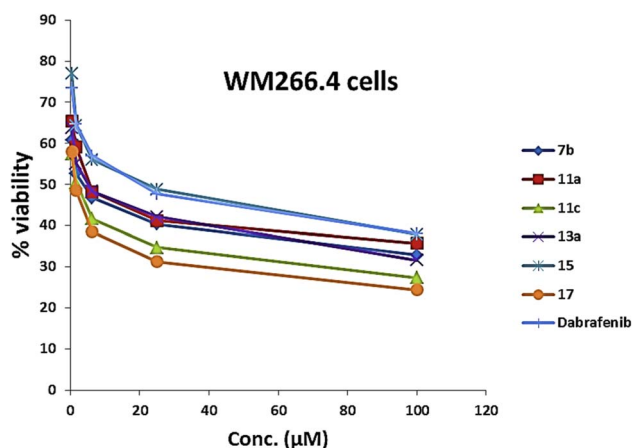Fig. 7 *In vitro* B-RAF wild type assay curves of compounds **7b**, **11c**, **13a**, **15**, **17**, and dabrafenib.

Fig. 8 Cytotoxicity assay curve of compounds **7b**, **11a** and **11c**, **13a**, **15**, **17**, and dabrafenib in B-RAFV600E-mutated WM266.4 melanoma cells.

(Scheme 5). The reaction of the latter with *p*-methoxyphenacyl bromide **18** afforded the corresponding fluorinated thiazole product **19**, as depicted in Scheme 5. Based on the spectroscopic data (experimental part), the structure of compound **19** was confirmed to be the *N*-[2-Benzenesulfonyl-1-(4-fluorophenyl)-ethylidene]-*N′*-[4-(4-methoxyphenyl)thiazol-2-yl]-hydrazine **19** (Scheme 5).

3.2.   Biological activity

3.2.1.   B-RAFV600E kinase assay. In this work, all target compounds were screened *in vitro* for their B-RAFV600E kinase inhibitory activity employing dabrafenib as the reference standard.

As presented in Table 1 and Fig. 6, all the tested compounds effectively inhibited the kinase activity of the B-RAFV600E enzyme with IC_{50} values at the nanomolar level in the range from 23.1 to 205 nM, which is equated to the reference drug dabrafenib ($IC_{50} = 47.2 \pm 2.5$ nM). Among the screened compounds, derivatives **7b** and **13a** revealed excellent B-
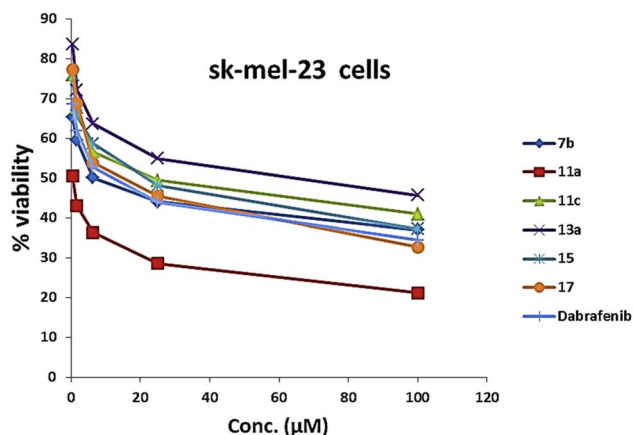
Fig. 9   Cytotoxicity assay curve of compounds **7b**, **11a** and **11c**, **13a**, **15**, **17**, and dabrafenib in B-RAF wild type Sk-mel-23 melanoma cells.

Table 2   The effect of compound **7b** on the phosphorylation of ERK in the WM266.4 cell line

Compound no.	pERK $1/2^a$ (ng mL^{-1})	% inhibition^b
7b	1.339 ± 0.035	51
Dabrafenib	0.769 ± 0.018	71.9
Control	2.732 ± 0.045	0

^{a} Data were expressed as mean $\pm$ standard error (S.E.) of two experiments. ^{b} Percentage of inhibition as compared with the control cancer cells.

RAFV600E inhibitory activity, superior to that of dabrafenib with IC$_{50}$ values of 36.3 ± 1.9, 23.1 ± 1.2, and 47.2 ± 2.5 nM, respectively. Furthermore, as expected, the bisthiazole derivative **15** showed potent B-RAFV600E inhibition (IC$_{50} = 51.9 \pm 2.7$ nM), nearly equipotent to that of dabrafenib. In addition, 70% of the activity of dabrafenib toward B-rafV600E was observed for compound **17** (IC$_{50} = 68.2 \pm 3.5$ nM). Meanwhile, compounds **3**, **7c**, **11a** and **11c**, and **19** displayed almost half the potency of dabrafenib with the IC$_{50}$ values ranging from 84.9 ± 4.4 to 116.3 ± 8 nM. In this investigation, derivatives **7a**, **11b**, and **13b** were the least potent against B-rafV600E kinase, exhibiting IC$_{50}$ values of about 200 nM.
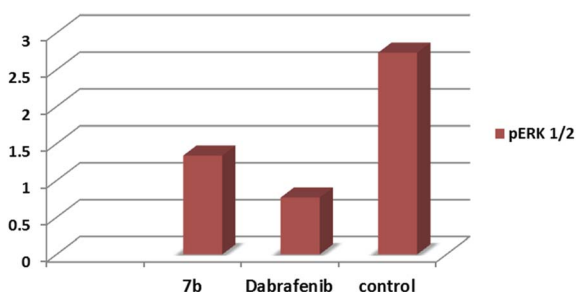

Fig. 10   The effect of compound **7b** on the phosphorylation of ERK in the WM266.4 cell line.

A brief investigation of the structure activity relationships revealed that, in general terms, arylazo thiazoles **7a–c** showed higher B-RAFV600E kinase inhibitory activity than aryl hydrazono thiazole derivatives **11a–c**. In addition, the tolyl derivatives **7b** and **7c** were much more potent than their unsubstituted phenyl analogue **7a** (IC$_{50} = 198.6 \pm 10$ nM). Besides, exceeding the activity of dabrafenib, the 3-tolyl analogue **7b** (IC$_{50} = 36.3 \pm 1.9$ nM) was 3-fold more active than its corresponding 4-tolyl derivative **7c** (IC$_{50} = 108.4 \pm 5.6$ nM). On the other hand, the unsubstituted phenyl **11a** and 4-nitrophenyl **11c** thiazolone derivatives possessed equipotent activity against B-RAFV600E kinase that was 2-fold higher than that elicited by their 4-chlorophenyl analogue **11b**.

Regarding compounds **13a** and **13b**, bearing the aryl moiety at the 4-position of thiazole nucleus, interestingly, the 4-bromophenyl analogue **13a** (IC$_{50} = 23.1 \pm 1.2$ nM) was the most potent among the tested compounds, displaying double the activity of dabrafenib. Conversely, the replacement of bromine atom in **13a** by a methyl group in derivative **13b** resulted in a dramatic decrease in the activity with compound **13b** (IC$_{50} = 205.6 \pm 11$ nM), being the least potent among the screened compounds.

3.2.2.   B-RAF wild-type kinase assay. To evaluate the selectivity of this series, the most potent compounds in B-RAFV600E kinase assay, namely, **7b**, **11a** and **11c**, **13a**, **15**, and **17** were further tested *in vitro* against B-RAF wild-type kinase. The results are depicted in Table 1 and Fig. 7. Noticeably, all the representative compounds showed a remarkable selectivity toward B-RAFV600E kinase, ranging from 2- to 5-fold, over the wild-type kinase. Compounds **7b**, **11a**, and **13a** were approximately four times more selective to B-RAFV600E kinase rather than the B-RAF wild-type kinase, while two-fold selectivity for B-RAFV600E kinase was observed for compounds **11c** and **17**. Among the tested compounds, derivative **15** inhibited B-RAF wild-type kinase at IC$_{50} = 251.2 \pm 13.5$ nM *versus* 51.9 ± 2.7 nM for the B-RAFV600E kinase, displaying 5-fold selectivity for B-RAFV600E kinase, similar to that elicited by the reference drug dabrafenib.

3.2.3.   Cytotoxicity against B-RAFV600E-mutated melanoma cells. To investigate the anticancer activity of the title compounds, the most potent derivatives, **7b**, **11a** and **11c**, **13a**, **15**, and **17** were screened against B-RAFV600E-mutated WM266.4 melanoma cells employing dabrafenib as the reference drug. All screened compounds potently inhibited the growth of WM266.4 melanoma cells with IC$_{50}$ values in the range from 1.24 to 17.1 μM, relative to dabrafenib (IC$_{50} = 16.5 \pm 0.91$ μM). Apart from compound **15** that was equipotent to dabrafenib, the rest of the tested compounds including **7b**, **11a** and **11c**, **13a**, and **17** were much more potent than the reference drug dabrafenib. Analogues **7b**, **11a**, and **13a** possessed remarkable anticancer activity against WM266.4 melanoma cells, three to five times more potent than that of dabrafenib. Moreover, with IC$_{50}$ values less than 2 μM, compounds **11c** and **17** revealed a significant cytotoxic effect toward WM266.4 melanoma cells, exceeding (11-fold) that of dabrafenib (Table 1 and Fig. 8).
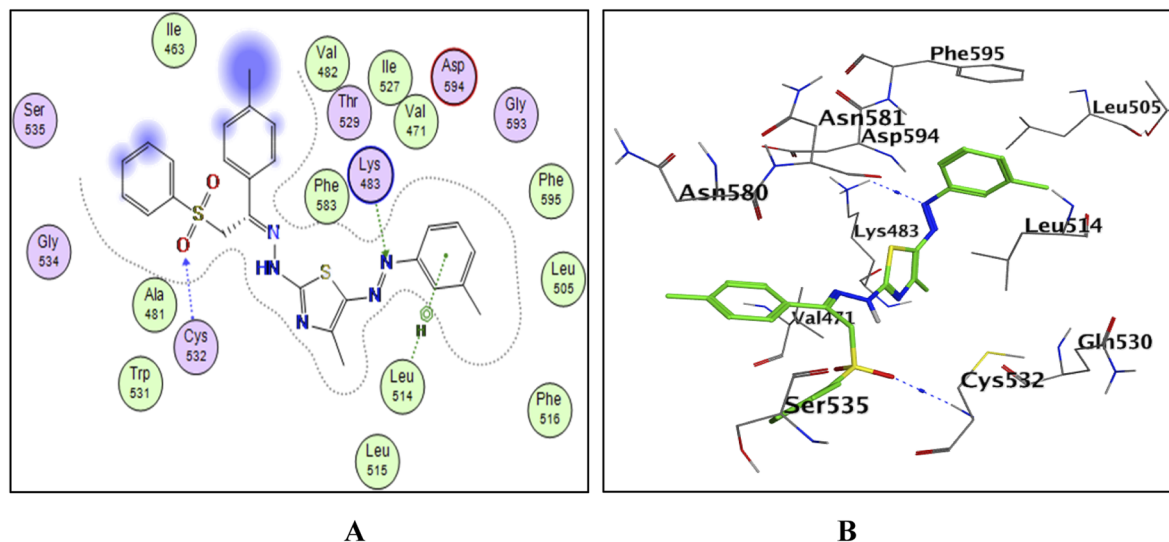
Fig. 11 The docked model of compound **7b** into the active site of the B–RAFV600E kinase; (A) 2D, (B) 3D.
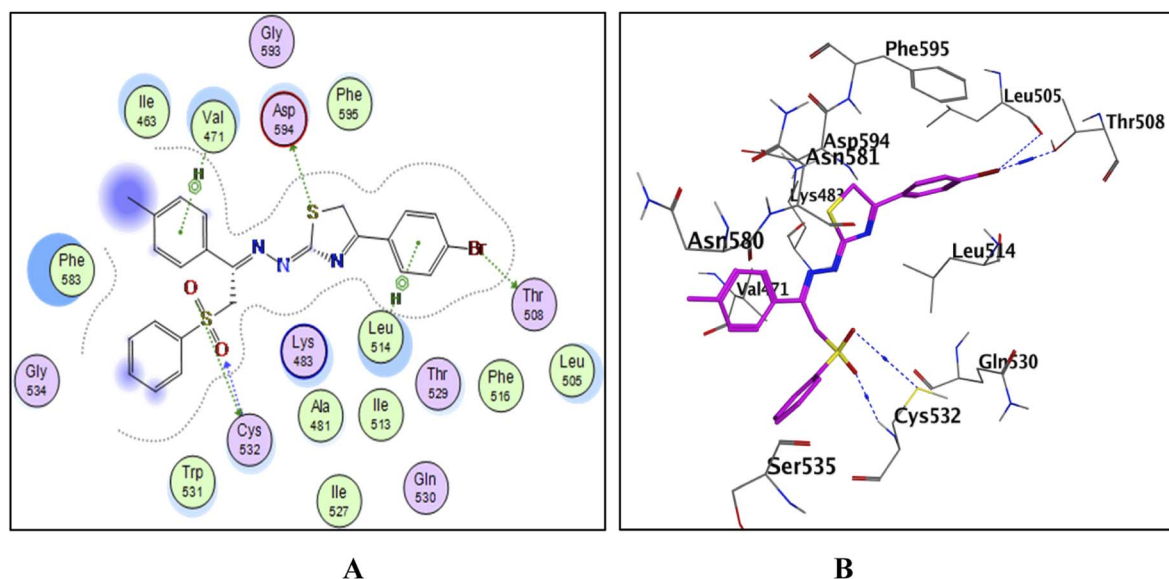

Fig. 12 The docked model of compound **13a** into the active site of the B–RAFV600E kinase; (A) 2D, (B) 3D.

3.2.4. Cytotoxicity against B-RAF wild type melanoma cells. The most potent derivatives, **7b**, **11a** and **11c**, **13a**, **15**, and **17** were further evaluated against human melanoma cells Sk-mel-23 (B-RAF wild type). As presented in Table 1 and Fig. 9, a positive correlation between the cytotoxic activity and selectivity for B-RAF V600E over B-RAF wild type was clearly observed for compounds **7b**, **11c**, **13a**, and **17**. Compound **7b** was approximately two times more potent against WM266.4 (B-RAFV600E-mutated) rather than Sk-mel-23 (B-RAF wild type) melanoma cells. Moreover, compounds **11c**, **13a**, and **17** were exceptionally more cytotoxic (10- to 15-fold) toward WM266.4 (B-RAFV600E-mutated) rather than Sk-mel-23 (B-RAF wild type) melanoma cells. Despite possessing high selectivity for B-

RAFV600E kinase over B-RAF wild type, bis compound **15** revealed equal potency against the two tested melanoma cells. On the other hand, among the tested compounds, compound **11a** was much more potent against Sk-mel-23 rather than WM266.4 melanoma cells.

3.2.5. Cell-based B-RAFV600E kinase assay. Furthermore, to link the B-RAFV600E kinase inhibitory activity with cell growth inhibition, an *in vitro* cell-based B-RAFV600E kinase assay was conducted. Thus, the blocking effect of compound **7b** was chosen as a representative of the most promising compounds on the phosphorylation of downstream ERK1/2 from WM266.4 (B-RAFV600E-mutated) melanoma cell line. As shown in Table 2 and Fig. 10, the treatment of WM266.4 cells
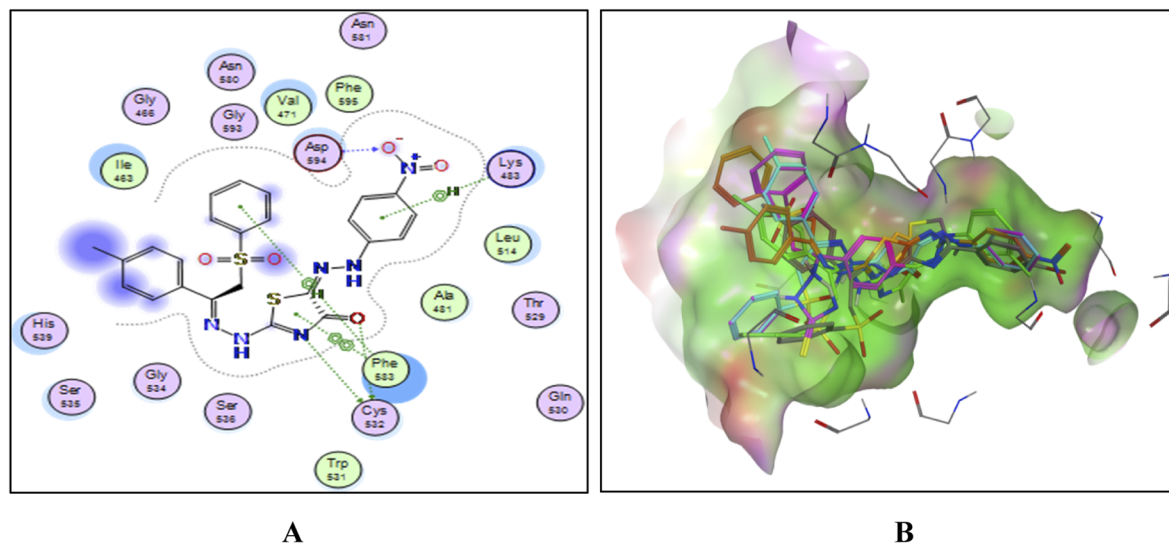
Fig. 13 (A) The 2D docked model of compound **11c** into the active site of the B-RAF V600E kinase, (B); overlay of the docked compounds into the active site of the B-RAF V600E kinase.

with compound **7b** resulted in approximately 51% reduction in the level of phosphorylated ERK1/2 *versus* 71.9% reduction for dabrafenib compared to untreated (control) cells.

3.3. Docking study

To explain the potent B-RAFV600E kinase inhibitory activity elicited by the title compounds on a molecular basis, a docking study of the most promising compounds in this work was performed using MOE (2014.0901). A high-resolution B-RAFV600E kinase enzyme co-crystallized with dabrafenib was retrieved form protein data bank (PDB code: 4XV2) to be used in the docking study.

Examining the docking results (Fig. 11–13) revealed good fitting and proper orientation of the docked compounds **7b**, **11a** and **11c**, **13a**, **15**, and **17** into the ATP binding site of B-RAFV600E kinase enzyme with docking energy scores of -8.99, -8.74, -8.80, -7.88, -8.68, and -5.01 kcal mol^{-1}, respectively, compared to the co-crystallized ligand dabrafenib (-9.95 kcal mol^{-1}). Despite showing more potent inhibitory activity against the B-RAF V600E kinase, the docking score of compound **13a** was relatively higher than that of compounds **7b**, **11a**, **11c**, and **15**. It is worth mentioning that inconsistencies between the inhibitory potency (experimental IC$_{50}$ values) and calculated docking scores have been reported.[51–53] Noticeably, all the analyzed compounds were involved in interactions with Cys532, a key residue in the hinge region of the enzyme active site. In addition, extensive hydrophobic interactions were observed between the docked compounds and Val471, Lys483, Leu505, Leu514, Phe583, and Phe595 residues, suggesting that the introduction of the hydrophobic groups (*e.g.*, aryl and arylazo) into the thiazole core enhanced the affinity of the target compounds to the ATP binding site of the B-RAFV600E enzyme. The previous molecular docking results combined with the data of the enzyme assay confirm that the title phenylsulfone–thiazole derivatives are potential inhibitors of BRAFV600E kinase (see the ESI† for more details).

4. Conclusion

To sum up, novel thiazole derivatives incorporating phenyl sulfonyl moiety were synthesized as the B-RAFV600E kinase inhibitors. All the target compounds inhibited the kinase catalytic activity of B-RAFV600E at nanomolar concentrations. Compounds **7b, 13a**, and **15** revealed excellent B-RAFV600E inhibitory activities, superior or equipotent to that of the reference drug dabrafenib. Furthermore, the title compounds were remarkably more selective toward B-RAFV600E kinase than the B-RAF wild-type. In addition, the newly synthesized compounds potently inhibited the growth of B-RAFV600E-mutated melanoma cells, showing more selectivity toward B-RAF V600E-mutated over B-RAF WT melanoma cells. A docking study also displayed hydrogen bonding and hydrophobic interactions of the title compounds with key residues within the active site of the B-RAFV600E kinase.

Conflicts of interest

There are no conflicts of interest to declare.

References

1 A. Plotnikov, E. Zehorai, S. Procaccia and R. Seger, The MAPK cascades: signaling components, nuclear roles and mechanisms of nuclear translocation, *Biochim. Biophys. Acta*, 2011, **1813**, 1619–1633.

2 Y. Sun, W.-Z. Liu, T. Liu, X. Feng, N. Yang and H.-F. Zhou, Signaling pathway of MAPK/ERK in cell proliferation, differentiation, migration, senescence and apoptosis, *J. Recept. Signal Transduction Res.*, 2015, **35**, 600–604.

3 T. Regad, Targeting RTK signaling pathways in cancer, *Cancers*, 2015, **7**, 1758–1784.

4 U. Degirmenci, M. Wang and J. Hu, Targeting aberrant RAS/RAF/MEK/ERK signaling for cancer therapy, *Cells*, 2020, **9**, 198.

5 T. Leicht, V. Balan, A. Kaplun, V. Singh-Gupta, L. Kaplun, M. Dobson and G. Tzivion, Raf kinases: function, regulation and role in human cancer, *Biochim. Biophys. Acta*, 2007, **1773**, 1196–1212.

6 H. Davies, G. R. Bignell, C. Cox, P. Stephens, S. Edkins, S. Clegg, J. Teague, H. Woffendin, M. J. Garnett and W. Bottomley, Mutations of the BRAF gene in human cancer, *Nature*, 2002, **417**, 949–954.

7 P. Rusconi, E. Caiola and M. Broggini, RAS/RAF/MEK inhibitors in oncology, *Curr. Med. Chem.*, 2012, **19**, 1164–1176.

8 H. B. El-Nassan, Recent progress in the identification of BRAF inhibitors as anti-cancer agents, *Eur. J. Med. Chem.*, 2014, **72**, 170–205.

9 J. J. Luke, K. T. Flaherty, A. Ribas and G. V. Long, Targeted agents and immunotherapies: optimizing outcomes in melanoma, *Nat. Rev. Clin. Oncol.*, 2017, **14**, 463–482.

10 P. Koelblinger, O. Thuerigen and R. Dummer, Development of encorafenib for BRAF-mutated advanced melanoma, *Curr. Opin. Oncol.*, 2018, **30**, 125–133.

11 B. Agianian and E. Gavathiotis, Current insights of BRAF inhibitors in cancer: miniperspective, *J. Med. Chem.*, 2018, **61**, 5775–5793.

12 H.-L. Li, M.-M. Su, Y.-J. Xu, C. Xu, Y.-S. Yang and H.-L. Zhu, Design and biological evaluation of novel triaryl pyrazoline derivatives with dioxane moiety for selective BRAFV600E inhibition, *Eur. J. Med. Chem.*, 2018, **155**, 725–735.

13 R. Buck, S. Saleh, M. I. Uddin and H. C. Manning, Rapid, microwave-assisted organic synthesis of selective V600EBRAF inhibitors for preclinical cancer research, *Tetrahedron Lett.*, 2012, **53**, 4161–4165.

14 A. Ayati, S. Emami, A. Asadipour, A. Shafiee and A. Foroumadi, Recent applications of 1, 3-thiazole core structure in the identification of new lead compounds and drug discovery, *Eur. J. Med. Chem.*, 2015, **97**, 699–718.

15 A. Ayati, S. Emami, S. Moghimi and A. Foroumadi, Thiazole in the targeted anticancer drug discovery, *Future Med. Chem.*, 2019, **11**, 1929–1952.

16 K. Mahmoud, T. A. Farghaly, H. G. Abdulwahab, N. T. Al-Qurashi and M. R. Shaaban, Novel 2-indolinone thiazole hybrids as sunitinib analogues: design, synthesis, and potent VEGFR-2 inhibition with potential anti-renal cancer activity, *Eur. J. Med. Chem.*, 2020, **208**, 112752.

17 M.-Y. Zhao, Y. Yin, X.-W. Yu, C. B. Sangani, S.-F. Wang, A.-M. Lu, L.-F. Yang, P.-C. Lv, M.-G. Jiang and H.-L. Zhu, Synthesis, biological evaluation and 3D-QSAR study of novel 4, 5-dihydro-1H-pyrazole thiazole derivatives as BRAFV600E inhibitors, *Bioorg. Med. Chem.*, 2015, **23**, 46–54.

18 M. Ammar, M. S. Abdel-Maksoud and C.-H. Oh, Recent advances of RAF (rapidly accelerated fibrosarcoma) inhibitors as anti-cancer agents, *Eur. J. Med. Chem.*, 2018, **158**, 144–166.

19 T. R. Rheault, J. C. Stellwagen, G. M. Adjabeng, K. R. Hornberger, K. G. Petrov, A. G. Waterson, S. H. Dickerson, R. A. Mook Jr, S. G. Laquerre and A. J. King, Discovery of dabrafenib: a selective inhibitor of Raf kinases with antitumor activity against B-Raf-driven tumors, *ACS Med. Chem. Lett.*, 2013, **4**, 358–362.

20 I. M. M. Othman, Z. M. Alamshany, N. Y. Tashkandi, M. A. M. Gad-Elkareem, S. S. Abd El-Karim and E. S. Nossier, Synthesis and biological evaluation of new derivatives of thieno-thiazole and dihydrothiazolo-thiazole scaffolds integrated with a pyrazoline nucleus as anticancer and multi-targeting kinase inhibitors, *RSC Adv.*, 2021, **12**, 561–577, DOI: 10.1039/d1ra08055e.

21 P. C. Sharma, K. K. Bansal, A. Sharma, D. Sharma and A. Deep, Thiazole-containing compounds as therapeutic targets for cancer therapy, *Eur. J. Med. Chem.*, 2020, **188**, 112016, DOI: 10.1016/j.ejmech.2019.112016.

22 H. S. Anbar, M. I. El-Gamal, H. Tarazi, B. S. Lee, H. R. Jeon, D. Kwon and C. H. Oh, Imidazothiazole-based potent inhibitors of V600E-B-RAF kinase with promising anti-melanoma activity: biological and computational studies, *J. Enzyme Inhib. Med. Chem.*, 2020, **35**, 1712–1726, DOI: 10.1080/14756366.2020.1819260.

23 U. M. Ammar, M. S. Abdel-Maksoud, E. Ali, K. I. Mersal, K. Ho Yoo and C. H. Oh, Structural optimization of imidazothiazole derivatives affords a new promising series as B-Raf V600E inhibitors; synthesis, in vitro assay and in silico screening, *Bioorg. Chem.*, 2020, **100**, 103967, DOI: 10.1016/j.bioorg.2020.103967.

24 T. A. Farghaly and M. M. Abdalla, Synthesis, tautomerism, antimicrobial, anti-HCV, anti-SSPE, antioxidant and antitumor activities of arylazobenzosuberones, *Bioorg. Med. Chem.*, 2009, **17**, 8012–8019.

25 T. A. Farghaly, H. G. Abdulwahab, H. Y. Medrasi, M. A. Al-Sheikh, D. F. Katowah and A. Alsaedi, Novel 6,7,8-trihydrobenzo[6',7']cyclohepta[2',1'-e]pyrazolo[2,3-a] pyrimidine derivatives as Topo IIα inhibitors with potential cytotoxic activity, *Bioorg. Chem.*, 2022, **128**, 106043, DOI: 10.1016/j.bioorg.2022.106043.

26 A. A. Gaber, M. Sobhy, A. Turky, H. G. Abdulwahab, A. A. Al-Karmalawy, M. A. Elhendawy, M. M. Radwan, E. B. Elkaeed, I. M. Ibrahim, H. Elzahabi and I. H. Eissa, Discovery of new 1H-pyrazolo[3,4-d]pyrimidine derivatives as anticancer agents targeting EGFR^{WT} and EGFR^{T790M}, *J. Enzyme Inhib. Med. Chem.*, 2022, **37**(1), 2283–2303, DOI: 10.1080/14756366.2022.2112575.

27 R. E. Mansour, H. G. Abdulwahab and H. El-Sehrawi, Novel mannich bases derived from 2-substituted benzimidazole and (thio) hydantoin moieties as potent histone deacetylase 6 (hdac6) inhibitors, *Azhar International Journal of Pharmaceutical and Medical Sciences*, 2021, **1**(3), 66–74, DOI: 10.21608/aijpms.2021.78337.1077.

28 S. A. Al-Hussain, T. A. Farghaly, M. E. Zaki, H. G. Abdulwahab, N. T. Al-Qurashi and Z. A. Muhammad, Discovery of novel indolyl-1, 2, 4-triazole hybrids as potent vascular endothelial growth factor receptor-2 (VEGFR-2) inhibitors with potential anti-renal cancer activity, *Bioorg. Chem.*, 2020, **105**, 104330.

29 Z. A. Muhammad, M. A. Radwan, T. A. Farghaly, H. M. Gaber and M. M. Elaasser, Synthesis and antitumor activity of novel [1, 2, 4, 5]-tetrazepino [6, 7-b] indole derivatives: marine

natural product Hyrtioreticuline C and D analogues, *Mini-Rev. Med. Chem.*, 2019, **19**, 79–86.

30 A. M. Gouda, H. A. El-Ghamry, T. M. Bawazeer, T. A. Farghaly, A. N. Abdalla and A. Aslam, Antitumor activity of pyrrolizines and their Cu (II) complexes: Design, synthesis and cytotoxic screening with potential apoptosis-inducing activity, *Eur. J. Med. Chem.*, 2018, **145**, 350–359.

31 A. M. Al-Soliemy, T. A. Farghaly, E. M. Abbas, M. R. Shaaban and M. E. Zayed, Synthesis of thiazolyl-*N*-phenylmorpholine derivatives and their biological activities, *Med. Chem.*, 2021, **17**, 790–805.

32 A. M. A. Alnaja, T. A. Farghaly, H. S. El-Zahabi and M. R. Shaaban, Cytotoxicity, docking study of new fluorinated fused pyrimidine scaffold: Thermal and microwave irradiation synthesis, *Med. Chem.*, 2021, **17**, 501–518.

33 I. Althagafi, N. M. El-Metwaly, M. G. Elghalban, T. A. Farghaly and A. M. Khedr, Synthesis of Pyrazolone Derivatives and Their Nanometer Ag (I) Complexes and Physicochemical, DNA Binding, Antitumor, and Theoretical Implementations, *Bioorg. Chem.*, 2018, **2018**, 1–15.

34 D. H. Dawood, E. M. Abbas, T. A. Farghaly, M. M. Ali and M. F. Ibrahim, ZnO nanoparticles catalyst in the synthesis of bioactive fused pyrimidines as anti-breast cancer agents targeting VEGFR-2, *Med. Chem.*, 2019, **15**, 277–286.

35 T. Farghaly, I. Abbas, W. Hassan, M. Lotfy, N. Al-Qurashi and T. B. Hadda, Structure Determination and Quantum Chemical Analysis of 1, 3-Dipolar Cycloaddition of Nitrile Imines and New Dipolarophiles and POM Analyses of the Products as Potential Breast Cancer Inhibitors, *Russ. J. Org. Chem.*, 2020, **56**, 1258–1271.

36 M. R. Shaaban, T. A. Farghaly and A. M. Alsaedi, Synthesis, Antimicrobial and Anticancer Evaluations of Novel Thiazoles Incorporated Diphenyl Sulfone Moiety, *Polycyclic Aromat. Compd.*, 2020, 1–17.

37 M. Grasso, M. A. Estrada, C. Ventocilla, M. Samanta, J. Maksimoska, J. Villanueva, J. D. Winkler and R. Marmorstein, Chemically Linked Vemurafenib Inhibitors Promote an Inactive BRAFV600E Conformation, *ACS Chem. Biol.*, 2016, **11**(10), 2876–2888, DOI: **10.1021/acschembio.6b00529**.

38 X.-H. Gu, X.-Z. Wan and B. Jiang, Syntheses and biological activities of bis(3-indolyl)thiazoles, analogues of marine bis(indole)alkaloid nortopsentins, *Bioorg. Med. Chem. Lett.*, 1999, **9**, 569–572, DOI: **10.1016/s0960-894x(99)00037-2**.

39 I. T. Radwan, A. H. M. Elwahy, A. F. Darweesh, M. Sharaky, N. Bagato, H. F. Khater and M. E. Salem, Design, synthesis, docking study, and anticancer evaluation of novel bis-thiazole derivatives linked to benzofuran or benzothiazole moieties as PI3k inhibitors and apoptosis inducers, *J. Mol. Struct.*, 2022, **1265**, 133454.

40 M. A. N. Mosselhi, M. A. Abdallah, Y. F. Mohamed and A. S. Shawali, Synthesis and Tautomeric Structure of 7-Arylhydrazono-7H-[1,2,4]Triazolo[3,4-b][1,3,4]Thiadiazines, *Phosphorus, Sulfur Silicon Relat. Elem.*, 2002, **177**, 487–498.

41 N. F. Eweiss and A. O. Osman, Synthesis of Heterocycles. Part II. New Routes to Acetylthiadiazolines and Alkylazothiazoles, *J. Heterocycl. Chem.*, 1980, **17**, 1713–1717.

42 M. A. Omar, G. S. Masaret, E. M. Abbas, M. M. Abdel-Aziz, M. F. Harras and T. A. Farghaly, Novel anti-tubercular and antibacterial based benzosuberone-thiazole moieties: Synthesis, molecular docking analysis, DNA gyrase supercoiling and ATPase activity, *Bioorg. Chem.*, 2020, **104**, 104316.

43 E. R. Cantwell-Dorris, J. J. O'Leary and O. M. Sheils, BRAFV600E: implications for carcinogenesis and molecular therapy, *Mol. Cancer Ther.*, 2011, **10**, 385–394.

44 N. M. Obaid, K. Bedard and W.-Y. Huang, Strategies for overcoming resistance in tumours harboring BRAF mutations, *Int. J. Mol. Sci.*, 2017, **18**, 585.

45 T. Mosdam, Rapid colorimetric assay for cellular growth and survival: Application to proliferation and cytotoxic assay, *J. Immunol. Methods*, 1983, **65**, 55–63.

46 M. M. Alsharekh, I. I. Althagafi, M. R. Shaaban and T. A. Farghaly, Microwave-assisted and thermal synthesis of nanosized thiazolyl-phenothiazine derivatives and their biological activities, *Res. Chem. Intermed.*, 2019, **45**, 127–154.

47 I. I. Althagafi, A. S. Abouzied, T. A. Farghaly, N. T. Al-Qurashi, M. Y. Alfaifi, M. R. Shaaban and M. R. Abdel Aziz, Novel Nano-sized bis-indoline Derivatives as Antitumor Agents, *J. Heterocycl. Chem.*, 2019, **56**, 391–399.

48 B. Gastaca, H. R. Sánchez, F. Menestrina, M. Caputo, M. de las Mercedes Schiavoni and J. J. P. Furlong, Thiosemicarbazones Synthesized from Acetophenones: Tautomerism, Spectrometric Data, Reactivity and Theoretical Calculations, *Int. J. Anal. Mass Spectrom. Chromatogr.*, 2019, **7**, 19–34.

49 D. Clemenceau, J. Cousseau, V. Martin, H. Molines, C. Wakselman, R. Mornet, F. Nogue and M. Laloue, Synthesis and cytokinin activity of two fluoro derivatives of N 6-isopentenyladenine, *J. Agric. Food Chem.*, 1996, **44**, 320–323.

50 O. V. El'kin, A. N. Bushuev, I. V. Tolstobrov, S. V. Fomin, E. S. Shirokova, A. V. Sazanov, V. A. Kozvonin and D. A. Kozulin, Organofluorine compounds in artificial blood circulation systems, *Fascinating Fluoropolym. Their Appl.*, 2020, 401–424.

51 S.-Y. Huang and X. Zou, Advances and Challenges in Protein-Ligand Docking, *Int. J. Mol. Sci.*, 2010, **11**(8), 3016–3034, DOI: **10.3390/ijms11083016**.

52 Y. C. Chen, Beware of docking!, *Trends Pharmacol. Sci.*, 2015 Feb, **36**(2), 78–95, DOI: **10.1016/j.tips.2014.12.001**.

53 C. Mikra, G. Rossos, S. K. Hadjikakou and N. Kourkoumelis, Molecular Docking and Structure Activity Relationship Studies of NSAIDs. What do they Reveal about IC50?, *Lett. Drug Des. Discovery*, 2017, **14**(8), 949–958, DOI: **10.2174/1570180814666161207143231**.